



The X-ray luminosity function of short gamma-ray bursts

Zhi-Ying Liu¹ · Fu-Wen Zhang^{1,2} · Si-Yuan Zhu¹

Received: 15 February 2021 / Accepted: 5 April 2021 / Published online: 12 April 2021
© The Author(s), under exclusive licence to Springer Nature B.V. 2021

Abstract We present for the first time the X-ray luminosity function of short gamma-ray bursts (sGRBs) estimated from 22 Fermi sGRBs. We find that the cumulative distribution of X-ray emission at rest frame 200 s is well described by a broken power law function, which is $\phi(L_{X,0}) \propto L_{X,0}^{-0.20 \pm 0.04}$ for dim bursts and $\phi(L_{X,0}) \propto L_{X,0}^{-1.05 \pm 0.11}$ for bright bursts, with the break luminosity is $2.57 \times 10^{46} \text{ erg s}^{-1}$, where the cosmological evolution of luminosity is taken into account. We also find that the early X-ray luminosity of sGRBs is correlated with the isotropic energy/luminosity of prompt emission. These results are need to confirm with large observed data of sGRBs.

Keywords Gamma-rays burst: general · Methods: statistical

1 Introduction

Gamma-ray bursts (GRBs) are the most dramatic explosions in the universe (see e.g., Piran 2004; Mészáros 2006; Zhang 2007). These events can be observed at a higher redshift than supernova(SNe), which are powerful tools for exploring the early universe (see e.g., Bromm and Loeb 2007; Zhang 2011; Wang et al. 2015). Traditionally, GRBs can be divided into two groups, long GRBs (IGRBs) and short GRBs (sGRBs), based on the well-known bimodal nature of the duration distribution with a separation at about $T_{90} \sim 2 \text{ s}$ (Kouveliotou et al. 1993). It is generally believed that some

IGRBs are associated with the deaths of massive stars (also called collapsars), while some sGRBs are produced by the merging of the binary compact objects (see e.g., Eichler et al. 1989; Narayan et al. 1992; Lipunov et al. 1995), such as neutron star—neutron star (NS-NS) and neutron star—black hole (NS-BH). The detection of gravitational wave event GW170817 associated with GRB 170817A, has confirmed that at least a fraction of the observed sGRBs are produced by the merger of binary neutron stars (Abbott et al. 2017). This also provide a new tool to study the nature of sGRBs.

The luminosity function ($\phi(L)$) is crucial constraint on the progenitor models. However, $\phi(L)$ cannot be derived straightforwardly using all GRBs with known redshifts since these samples are affected by observational bias. Some studies have estimated the luminosity function assuming the function form and fitting the data to derive model parameters (see e.g., Salvaterra and Chincarini 2007; Salvaterra et al. 2009). In this approach, the results seriously depend on the functional form of the model. On the other hand, based on the observed samples of GRBs with measured z and L , the luminosity function can be directly derived. The Lynden-Bell c^- method is an efficient method to determine the distribution of the luminosity function of astronomical objects with a truncated sample. This method was first used to estimate the luminosity function of galaxies and quasars (see e.g., Lynden-Bell 1971; Efron and Petrosian 1992; Petrosian 1993; Kirshner et al. 1978; Loh and Spillar 1986; Peterson et al. 1986), and then it is extensively adopted to GRBs (see e.g., Lloyd-Ronning et al. 2002; Yonetoku et al. 2004, 2014; Wu et al. 2012; Yu et al. 2015; Pescalli et al. 2016; Zhang and Wang 2018). Recently, Wang et al. (2013) and Cui et al. (2014) have studied the luminosity function of GRB optical afterglow. However, the luminosity function of GRB X-ray

✉ F.-W. Zhang
fwzhang@pmo.ac.cn

¹ College of Science, Guilin University of Technology, Guilin 541004, China

² Key Laboratory of Dark Matter and Space Astronomy, Chinese Academy of Sciences, Nanjing 210008, China

emission has not studied so far, especially, the properties of sGRBs are need to explore.

In this paper, we for the first time study the early X-ray afterglow luminosity function of Fermi sGRBs using the Lynden-Bell c^- method. This paper is organized as follows. In Sect. 2, we introduce our sample and data selection. In Sect. 3, we introduce the early X-ray afterglow luminosity function of Fermi sGRBs. Finally, we give our conclusions and discussion in Sect. 4. Throughout this paper, we adopt the standard flat cold dark matter cosmology with the typical cosmological parameters $\Omega_m = 0.27$ and $H_0 = 70 \text{ km s}^{-1} \text{ Mpc}^{-1}$.

2 sGRB sample and data analysis

We concentrate our analysis on the sGRBs detected only by the Fermi detector to minimize the influence of different instruments (with different sensitivities and energy bands). The Fermi GRBs are selected from the Fermi catalog¹ until the end of January 2020. In total, there are 2698 events. First, according to the traditional sGRB definition method ($T_{90} < 2 \text{ s}$), we select the bursts with well-measured spectral parameters and their durations are less than 2 seconds, in total there are 367 events. In addition, GRB 100816A with a duration of 2.045 s was classified as sGRB shown in Xue et al. (2019), and is included in our sample. Our Fermi sample thus contains 368 sGRBs. To study the X-ray afterglow of sGRBs, the X-ray emission data observed by the Swift X-ray Telescope (XRT) are taken.² Only 34 short bursts have X-ray data as shown in Fig. 1.

In this paper, we mainly use the data of the early decay phase afterglow to study the X-ray luminosity function. In addition, we define the rest frame time $T_a^* = 200 \text{ s}$ (the symbol * represents the value in the rest-frame) as the time point. The sGRBs must have the X-ray data both before and after T_a^* , thereby allowing an interpolation to T_a^* . Among these bursts, GRB 081101, GRB 090621B, GRB 140209A, GRB 150101B, GRB 151228A and GRB 160411A have no the early decay phase afterglow data. GRB 090531B, GRB 100206A, GRB 111222A, GRB 140402A and GRB 150101A have only one data point. The afterglow of GRB 131004A at $T_a^* = 200 \text{ s}$ is in the plateau phase, not in the decay phase. These bursts are excluded from our sample. Finally, our sample consists of 22 Fermi sGRBs. In Table 1, we list the properties of 22 sGRBs with the X-ray afterglows, including the burst name, redshift z , the observer frame time T_a corresponding to the rest frame 200 s, the flux F_X in the 0.3-10 keV at the time T_a , the energy spectrum index

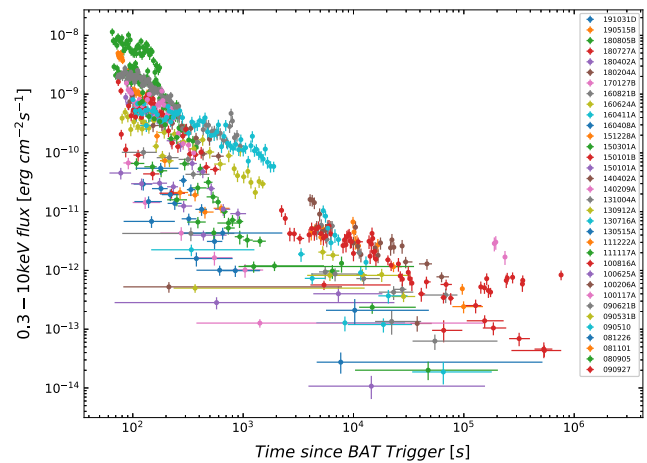


Fig. 1 X-ray light curves of 34 Fermi sGRBs

β_a , isotropic X-ray luminosity L_X . The X-ray luminosity of sGRB can be derived with the following equation (Dainotti et al. 2011),

$$L_X = \frac{4\pi D_L^2(z) F_X}{(1+z)^{1-\beta_a}}, \quad (1)$$

where D_L is the luminosity distance, F_X is the 0.3-10 keV flux observed at time $T_a^* = 200 \text{ s}$, β_a is the energy spectrum index corresponding to the X-ray afterglow at time T_a . If there is no F_X data at the time T_a , we adopt the interpolated method to estimate F_X . Here we describe simply the X-ray light curve near the time T_a as a power-law decay ($F_X \propto t^\alpha$), and then fit the data before and after T_a to estimate the flux F_X at the time T_a .

In fact, the number of Fermi sGRBs with measured redshifts and X-ray afterglow data is very small. In our sample, only 8 bursts have redshifts. In order to calculate the X-ray luminosity, the values of sGRB redshifts are needed. Previous authors have estimated the pseudo redshifts of sGRBs using the $L_p - E_p$ correlations between the peak luminosity L_p and the rest frame peak energy E_p (Yonetoku et al. 2014; Zhang and Wang 2018). We also use this method to estimate the pseudo redshifts of Fermi sGRBs with unknown redshifts. In Paper 1 we have collected 22 sGRBs with known redshifts and well measured spectra to analyzed the $L_p - E_p$ correlation, and found that $L_p/10^{51} = (-4.91 \pm 0.89)(E_p)^{1.90 \pm 0.31}$, with the correlation coefficient $r = 0.81$. We can rewrite the equation as

$$\frac{D_L^2(z)}{(1+z)^{1.90}} = \frac{10^{46.09}}{4\pi F_p} \left(\frac{E_p}{\text{keV}} \right)^{1.90}. \quad (2)$$

Using the Equation 2 we derive the pseudo redshifts of 14 Fermi sGRBs with unknown redshifts, and then derive their X-ray luminosity as described above. The results are shown in Table 1. In Fig. 2, we present the X-ray luminosity distribution of sGRBs.

¹<https://heasarc.gsfc.nasa.gov/W3Browse/fermi/fermigbrst.html>.

²https://www.swift.ac.uk/burst_analyser/?tdsourcetag=s_ptcim_aiomsg.

Table 1 X-ray properties of 22 Fermi sGRBs

GRB	z	T_a s	F_X $10^{-11} \text{ erg cm}^{-2} \text{ s}^{-1}$	β_a	L_X $10^{46} \text{ erg s}^{-1}$
191031D	0.279 ^a	255.8	1.26 ± 0.31	0.85 ± 0.21	0.30 ± 0.07
190515B	0.785 ^a	357.0	1.65 ± 0.42	1.68 ± 0.25	7.25 ± 1.84
180805B	0.473 ^a	294.6	30.21 ± 5.58	-0.23 ± 0.37	16.12 ± 2.98
180727A	0.187 ^a	237.4	1.39 ± 0.391	0.58 ± 0.25	0.13 ± 0.04
180402A	0.52 ^a	304.0	8.91 ± 1.49	0.44 ± 0.33	7.61 ± 1.27
180204A	0.379 ^a	275.8	25.55 ± 6.43	1.13 ± 0.32	13.47 ± 3.39
170127B	0.59 ^a	318.0	0.36 ± 0.11	0.52 ± 0.22	0.43 ± 0.13
160821B	0.16	232.0	59.31 ± 10.11	1.53 ± 0.21	4.53 ± 0.77
160624A	0.483	296.6	2.12 ± 0.01	0.65 ± 0.23	1.67 ± 0.01
160408A	0.671 ^a	334.2	2.42 ± 0.53	1.06 ± 0.20	5.02 ± 1.10
150301A	0.445 ^a	289.0	42.28 ± 5.31	0.15 ± 1.18	22.93 ± 2.88
130912A	0.685 ^a	337.0	14.21 ± 2.66	0.41 ± 0.24	22.13 ± 4.14
130716A	1.019 ^a	403.8	1.65 ± 0.05	1.21 ± 0.33	10.88 ± 0.33
130515A	0.305 ^a	261.0	0.28 ± 0.04	0.63 ± 0.83	0.08 ± 0.01
111117A	2.211	644.2	0.72 ± 0.12	0.63 ± 0.18	18.19 ± 3.01
100816A	0.8049	360.98	9.33 ± 2.00	0.68 ± 0.28	24.40 ± 5.23
100625A	0.452	290.4	1.43 ± 0.27	1.11 ± 0.19	1.14 ± 0.22
100117A	0.92	384.0	4.05 ± 2.24	1.44 ± 0.23	23.76 ± 13.12
090621B	0.53 ^a	306.0	0.45 ± 0.11	2.16 ± 0.65	0.83 ± 0.21
090510	0.903	380.6	29.16 ± 6.38	0.74 ± 0.24	103.73 ± 22.68
081226	0.827 ^a	365.4	1.35 ± 0.99	2.36 ± 0.68	10.34 ± 7.55
080905	1.505	501.0	1.61 ± 0.41	0.71 ± 0.24	18.54 ± 4.67

^aThese sGRBs have pseudo redshifts

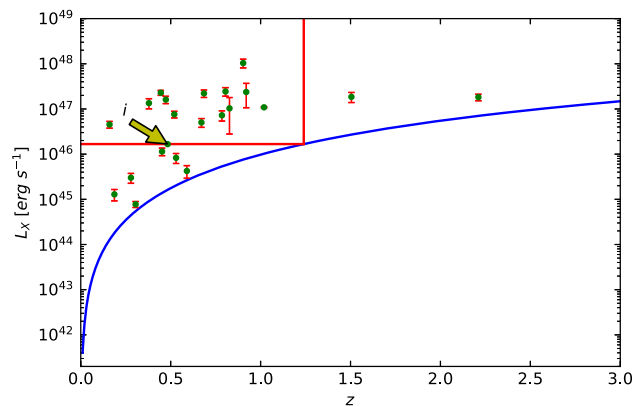


Fig. 2 X-ray luminosity distribution of 22 Fermi sGRBs. The blue line represents the observational limit of $1.8 \times 10^{46} \text{ erg cm}^{-2} \text{ s}^{-1}$

3 The luminosity function of X-ray afterglows of sGRBs

The Lynden-Bell c^- method is an effective method for determining the luminosity and redshift distribution of truncated data sample, including quasars (see e.g., Lynden-Bell

1971; Efron and Petrosian 1992; Petrosian 1993), galaxies (see e.g., Kirshner et al. 1978; Loh and Spillar 1986; Peterson et al. 1986), and GRBs (see e.g., Lloyd-Ronning et al. 2002; Yonetoku et al. 2004, 2014; Wu et al. 2012; Yu et al. 2015; Pescalli et al. 2016; Zhang and Wang 2018).

The luminosity function $\Psi(L, z)$ is correlated to the two quantities of luminosity and redshift. In general, luminosity is correlated to redshift, so we can not simply write the luminosity function into $\Psi(L, z) = \phi(L)\rho(z)$. We need firstly to remove the redshift evolution of luminosity. Therefore, we rewrite the luminosity function as $\Psi(L, z) = \rho(z)\phi(L/g_k(z))/g_k(z)$, where $\phi(L/g_k(z))$ is the local (at $z = 0$) luminosity function, and $g_k(z)$ accounts for the evolution of L . Then, the luminosity at redshift $z = 0$ is $L_0 = L/g_k(z)$, and L_0 is independent of z . The goal of our analysis is to obtain the local luminosity function $\phi(L_0)$.

Firstly, we need to remove the effect of the luminosity evolution and determine the value of k by assuming a evolution functional form of $g_k(z) = (1 + z)^k$ as done by many previous works (Lloyd-Ronning et al. 2002; Yonetoku et al. 2014; Yu et al. 2015; Zhang and Wang 2018; Guo et al. 2020). Following Efron and Petrosian (1992), we use the

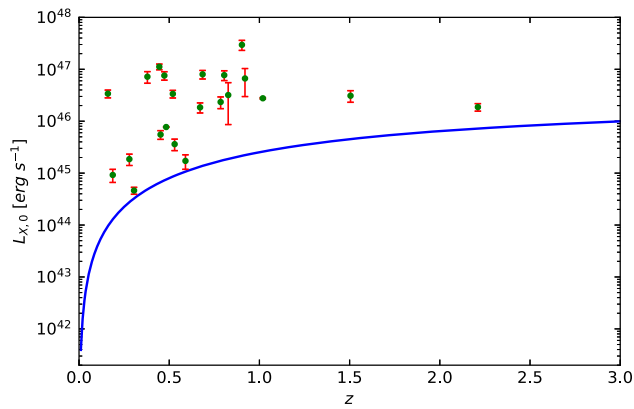


Fig. 3 Non-evolving X-ray luminosity distribution of 22 Fermi sGRBs

non-parametric test method of an τ statistical method to derive the value of k .

In the (L_X, z) plane as shown in Fig. 2, for a random point of i th $(L_{X,i}, z_i)$, we can consider an associated set J_i as

$$J_i = \{j | L_{X,j} \geq L_{X,i}, z_j \leq z_i^{\max}\}, \quad (3)$$

where $L_{X,i}$ is the X-ray luminosity of i th sGRB and z_i^{\max} is the maximum redshift at which the sGRBs with the X-ray luminosity $L_{X,i}$ can be detected by the Swift detector. This range is the red region of Fig. 2. We define the number of sGRBs contained in this region as N_i . In addition, the blue solid line in Fig. 2 represents the observed flux limit, $F_{X,\text{limit}} = 1.8 \times 10^{-12} \text{ erg cm}^{-2} \text{ s}^{-1}$.

If L_X and z are independent of each other, one would expect the number R_i , $R_i = \text{Number}\{j \in J_i | z_j \leq z_i\}$, is uniformly distributed between 1 and N_i . The test statistic τ is

$$\tau = \frac{\sum_i (R_i - E_i)}{\sqrt{\sum_i V_i}}, \quad (4)$$

where $E_i = (N_i + 1)/2$ and $V_i = (N_i^2 - 1)/12$ are the expected mean and the variance of R_i , respectively. If R_i follows an ideal uniform distribution, then the samples of $R_i \geq E_i$ and $R_i \leq E_i$ should be equal, and the value of τ should be equal to zero. However, L_X and z are not independent of each other. We change the value of k until the test statistic τ is zero. We find that the best fitting is $k = 1.95^{+1.12}_{-1.08}$. The distribution of non-evolving X-ray luminosity $L_{X,0}$ is shown in Fig. 3.

After removing the effect of the X-ray luminosity evolution through $L_{X,0} = L_X / (1 + k)^{1.95}$, we can use the non-parametric method to derive the cumulative X-ray luminosity function $\phi(L_{X,0})$ from the following equation

$$\phi(L_{X,0,i}) = \prod_{j < i} \left(1 + \frac{1}{N_j}\right), \quad (5)$$

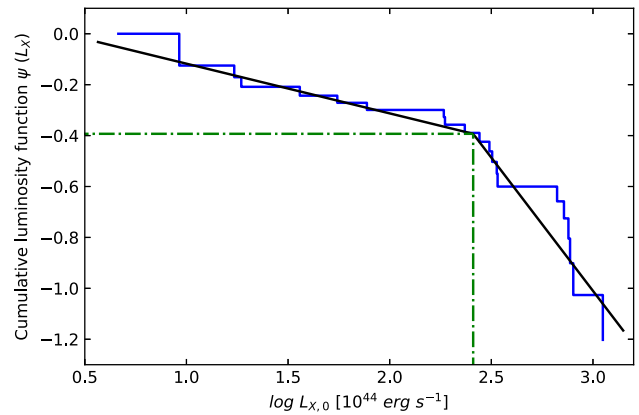


Fig. 4 Cumulative X-ray luminosity function of sGRBs, which is normalized to unity at the lowest luminosity. The black line is the best fit with a broken power-law model. The X-ray luminosity function can be expressed as $\phi(L_{X,0}) \propto L_{X,0}^{-0.20 \pm 0.04}$ for dim bursts and $\phi(L_{X,0}) \propto L_{X,0}^{-1.05 \pm 0.11}$ for bright bursts, with a break luminosity of $L_{X,0}^b = 2.57 \times 10^{46} \text{ erg s}^{-1}$

where $j < i$ means that the j th burst has a larger X-ray luminosity than i th one. Figure 4 shows the cumulative X-ray luminosity function. The shape of luminosity function follows a broken power-law, and the best fitting is given by

$$\phi(L_{X,0}) \propto \begin{cases} L_{X,0}^{-0.20 \pm 0.04}, & L_{X,0} < L_{X,0}^b \\ L_{X,0}^{-1.05 \pm 0.11}, & L_{X,0} \geq L_{X,0}^b \end{cases}, \quad (6)$$

where the break luminosity $L_{X,0} = 2.57 \times 10^{46} \text{ erg s}^{-1}$. It is worth noting that the X-ray luminosity function here corresponds to $z = 0$, and the X-ray luminosity function of sGRBs at redshift z is $\phi(L_{X,0})(1 + z)^{1.95}$.

4 Results and discussion

Using the 22 Fermi sGRBs with the early X-ray afterglow emission, we construct the X-ray luminosity function of sGRBs at rest frame 200 s after the burst onset. Considering the redshift evolution of X-ray luminosity, we adopt the Lynden-Bell c^- method to study the X-ray luminosity function of sGRBs. After removing the effects of luminosity evolution, we find that the cumulative luminosity function can be fitted with a broken power-law function, $\phi(L_{X,0}) \propto L_{X,0}^{-0.20 \pm 0.04}$ for dim bursts and $\phi(L_{X,0}) \propto L_{X,0}^{-1.05 \pm 0.11}$ for bright bursts, where the break X-ray luminosity is $2.57 \times 10^{46} \text{ erg s}^{-1}$. This is a preliminary result, which need to confirm with large sGRB sample in the future. Note that due to the limitations of the observations, we only analyze the data from the small sample, and there is indeed some selection effect. We compare the redshift distribution and the fluence distribution of our sample with those of the

Table 2 Prompt emission properties of 22 Fermi sGRBs with the measured early X-ray afterglow

GRB	z	T_{90} s	α	E_p keV	F_p $10^{-6} \text{ erg cm}^{-2} \text{ s}^{-1}$	S_γ $10^{-7} \text{ erg cm}^{-2}$	e_{min} keV	e_{max} keV	L_p $10^{51} \text{ erg s}^{-1}$	E_{iso} 10^{51} erg
191031D	0.279 ^a	0.256 ± 0.023	-0.42 ± 0.04	856.00 ± 53.00	48.70 ± 1.59 ^b	43.60 ± 0.90	10	1000	1.24 ± 0.03	7.37 ± 0.241
190515B	0.785 ^a	1.264 ± 0.471	-0.40 ± 0.20	960.00 ± 251.00	8.20 ± 9.00 ^b	12.33 ± 0.70	10	1000	3.29 ± 0.19	17.16 ± 1.88
180805B	0.473 ^a	0.960 ± 0.590	-0.50 ± 0.20	346.00 ± 75.00	8.30 ± 1.10 ^b	5.90 ± 0.70	10	1000	0.36 ± 0.04	1.72 ± 0.23
180727A	0.187 ^a	0.896 ± 0.286	0.14 ± 0.28	69.00 ± 4.00	7.20 ± 1.20 ^b	3.32 ± 0.18	10	1000	0.029 ± 0.002	0.054 ± 0.009
180402A	0.52 ^a	0.448 ± 0.326	-0.37 ± 0.09	1326.79 ± 152.34	10.21 ± 0.72	18.18 ± 0.79	10	1000	2.75 ± 0.12	23.46 ± 1.65
180204A	0.379 ^a	1.152 ± 0.091	-0.88 ± 0.06	852.88 ± 146.05	11.33 ± 0.68	26.63 ± 0.94	10	1000	1.44 ± 0.05	8.43 ± 0.50
170127B	0.59 ^a	1.728 ± 1.346	-0.43 ± 0.18	621.91 ± 120.49	3.35 ± 0.41	7.08 ± 0.59	10	1000	0.80 ± 0.07	6.04 ± 0.73
160821B	0.16	1.088 ± 0.977	-1.40 ± 0.25	91.97 ± 27.87	0.95 ± 0.21	1.66 ± 0.25	10	1000	0.012 ± 0.002	0.081 ± 0.018
160624A	0.483	0.384 ± 0.405	-0.62 ± 0.21	1153.31 ± 488.47	2.95 ± 0.48	5.26 ± 0.49	10	1000	0.58 ± 0.05	4.85 ± 0.79
160408A	0.671 ^a	1.056 ± 0.604	-0.72 ± 0.10	890.10 ± 152.06	4.33 ± 0.44	12.77 ± 0.61	10	1000	2.32 ± 0.11	13.15 ± 1.35
150301A	0.445 ^a	0.416 ± 0.295	-0.63 ± 0.40	191.09 ± 59.09	0.71 ± 0.12	1.24 ± 0.26	10	1000	0.065 ± 0.013	0.54 ± 0.133
130912A	0.685 ^a	0.512 ± 0.143	-1.00 ± 0.10	998.16 ± 234.70	4.90 ± 0.45	11.59 ± 0.62	10	1000	2.34 ± 0.12	16.64 ± 1.51
130716A	1.019 ^a	0.768 ± 0.389	-0.48 ± 0.23	818.94 ± 381.37	1.97 ± 0.62	7.35 ± 0.89	10	1000	2.97 ± 0.36	16.10 ± 5.00
130515A	0.305 ^a	0.256 ± 0.091	-0.32 ± 0.15	496.48 ± 59.98	7.99 ± 0.69	10.75 ± 0.72	10	1000	0.28 ± 0.02	2.71 ± 0.24
111117A	2.211	0.432 ± 0.082	-0.50 ± 0.17	543.62 ± 102.96	2.98 ± 0.42	6.82 ± 0.60	10	1000	9.66 ± 0.853	135.32 ± 19.11
100816A	0.8049	2.045 ± 0.229	-0.37 ± 0.07	140.07 ± 6.07	1.48 ± 0.06	33.548 ± 1.10	10	1000	5.97 ± 0.20	4.77 ± 0.18
100625A	0.452	0.240 ± 0.276	-0.59 ± 0.13	483.19 ± 63.32	5.97 ± 0.79	12.70 ± 0.96	10	1000	0.76 ± 0.06	5.17 ± 0.69
100117A	0.92	0.256 ± 0.834	-0.10 ± 0.26	325.43 ± 51.09	1.73 ± 0.39	3.72 ± 0.57	10	1000	0.87 ± 0.133	7.77 ± 1.74
090621B	0.53 ^a	0.384 ± 1.032	-0.10 ± 0.29	519.28 ± 97.86	3.15 ± 0.59	4.90 ± 0.55	10	1000	0.41 ± 0.05	3.99 ± 0.75
090510	0.903	0.960 ± 0.138	-0.86 ± 0.02	4727.06 ± 348.98	18.29 ± 0.78	44.22 ± 1.05	10	1000	60.33 ± 1.43	474.99 ± 20.13
081226	0.827 ^a	0.832 ± 1.032	-0.81 ± 0.19	583.49 ± 188.19	1.69 ± 0.49	4.61 ± 0.71	10	1000	1.04 ± 0.16	6.97 ± 2.03
080905	1.505	0.960 ± 0.345	0.20 ± 0.73	349.71 ± 55.27	2.87 ± 0.45	4.48 ± 0.59	10	1000	2.74 ± 0.36	43.99 ± 6.94

^aThese sGRBs have pseudo redshifts

^bFor these sGRBs, the peak flux is in units of photons $\text{cm}^{-2} \text{ s}^{-1}$

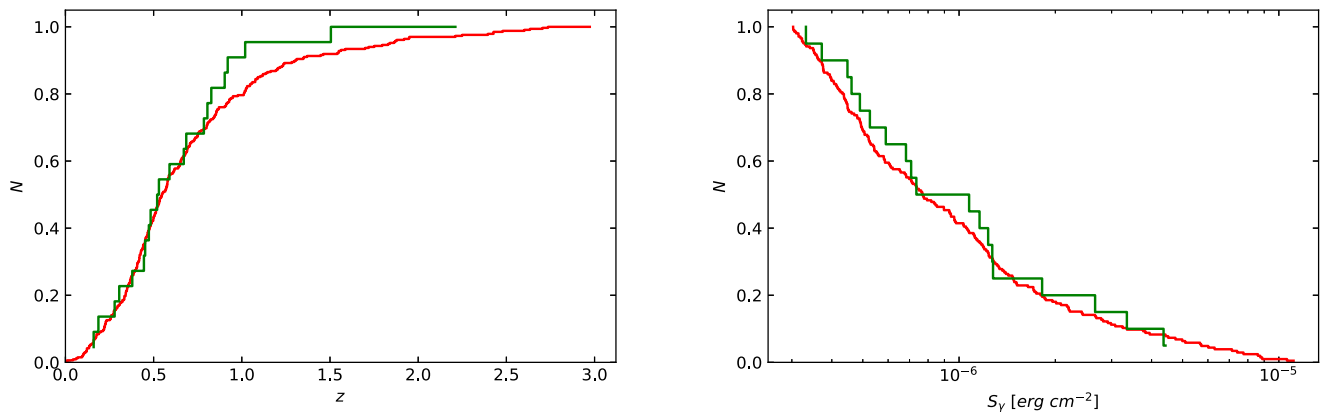


Fig. 5 Comparisons of the redshift distribution (left panel) and the fluence distribution (right panel) of our sample (green) with those of the overall Fermi sGRBs (red), where the redshifts of the overall Fermi

sGRBs with unknown redshift are estimated using the same $L_p - E_p$ correlation. The p values of Kolmogorov-Smirnov test are 0.92 and 0.90, respectively

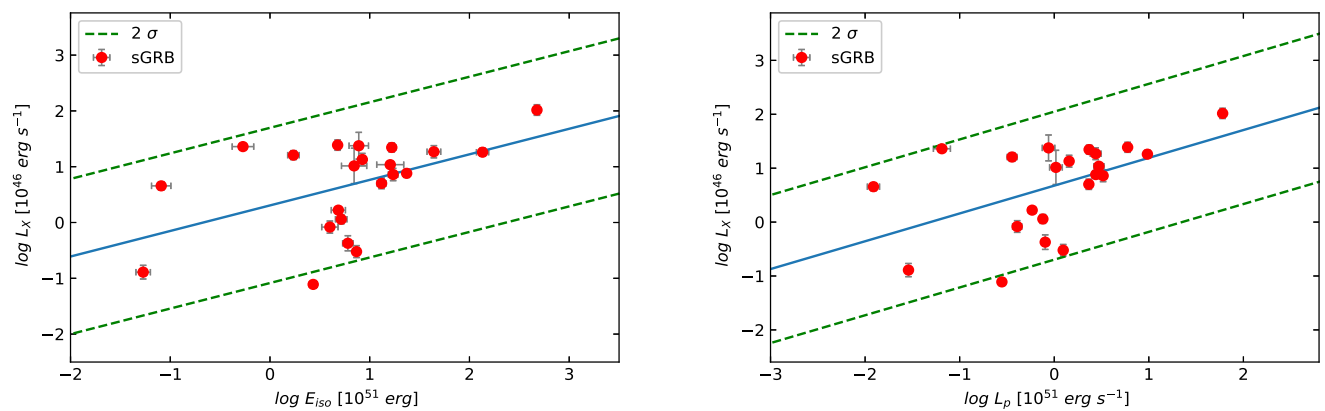


Fig. 6 Relations between the early X-ray afterglow luminosity and the isotropic energy/luminosity of the prompt emission for sGRBs. The left panel shows the $L_X - E_{\text{iso}}$ correlation, the $L_X - L_p$ correlation is

displayed in the right panel. The blue solid lines are the best fits. The green dotted line is the 2σ prediction band

overall Fermi sGRBs, and the results are shown in Fig. 5. From this figure, one can see the distributions of both are basically the same. We also perform the Kolmogorov-Smirnov test, the p values are 0.92 and 0.90, respectively. In addition, the Fermi threshold is also affect the result. The bursts with high redshift and low luminosity can not be observed, the number of low luminosity sGRBs should be underestimated.

We also further analyze the correlations between the isotropic energy (E_{iso})/luminosity(L_p) of the prompt emission and the X-ray luminosity of sGRBs. The results are shown in Table 2 and Fig. 6. From this figure, we can see that the early decay phase X-ray luminosity of sGRBs is correlated with the prompt isotropic energy/luminosity. For the $L_X - E_{\text{iso}}$ correlation, the best fit is $\log L_X = (0.13 \pm 0.22) + (0.45 \pm 0.18) \log E_{\text{iso}}$. The correlation coefficient r is 0.49, with a chance probability $p = 0.00015$ and the dispersion $\sigma = 0.51$. For the $L_X - L_p$ correlation, the best fit is $\log L_X = (0.68 \pm 0.16) + (0.52 \pm 0.20) \log L_p$, with

$r = 0.51$, $p < 10^{-4}$, and $\sigma = 0.82$. These results indicate that the early decay phase X-ray emission of sGRBs are mainly dominated by the prompt emission.

Acknowledgements We acknowledgment the use of public data from the Fermi and Swift catalogue. This work was supported in part by NSFC under grants 11763003, and by the Guangxi Natural Science Foundation (No. 2017GXNSFAA198094).

Publisher’s Note Springer Nature remains neutral with regard to jurisdictional claims in published maps and institutional affiliations.

References

Abbott, B.P., Abbott, R., Abbott, T.D., et al.: Phys. Rev. Lett. **119**, 161101 (2017)
 Bromm, V., Loeb, A.: (2007). [arXiv:0706.2445](https://arxiv.org/abs/0706.2445)
 Cui, X.H., Wu, X.F., Wei, J.J., et al.: Astrophys. J. **795**, 103 (2014)
 Dainotti, M.G., Willingale, R., Capozziello, S., et al.: American Institute of Physics Conference Series, vol. 113 (2011)
 Efron, B., Petrosian, V.: Astrophys. J. **399**, 345 (1992)

- Eichler, D., Livio, M., Piran, T., et al.: *Nature* **340**, 126 (1989)
- Guo, Q., Wei, D.-M., Wang, Y.-Z., et al.: *Astrophys. J.* **896**, 83 (2020)
- Kirshner, R.P., Oemler, A.J., Schechter, P.L.: *Astron. J.* **83**, 1549 (1978)
- Kouveliotou, C., Meegan, C.A., Fishman, G.J., et al.: *Astrophys. J. Lett.* **413**, L101 (1993)
- Lipunov, V.M., Postnov, K.A., et al.: *J. Astrophys.* **454**, 593 (1995)
- Lloyd-Ronning, N.M., Fryer, C.L., Ramirez-Ruiz, E.: *Astrophys. J.* **574**, 554 (2002)
- Loh, E.D., Spillar, E.J.: *Astrophys. J. Lett.* **308**, L1 (1986)
- Lynden-Bell, D.: *Mon. Not. R. Astron. Soc.* **155**, 95 (1971)
- Mészáros, P.: *Reports on Progress in Physics* **69**, 2259 (2006)
- Narayan, R., Paczynski, B., Piran, T.: *Astrophys. J. Lett.* **395**, L83 (1992)
- Pescalli, A., Ghirlanda, G., Salvaterra, R., et al.: *Astron. Astrophys.* **587**, A40 (2016)
- Peterson, B.A., Ellis, R.S., Efstathiou, G., et al.: *Mon. Not. R. Astron. Soc.* **221**, 233 (1986)
- Petrosian, V.: *Astrophys. J. Lett.* **402**, L33 (1993)
- Piran, T.: *Reviews of Modern Physics* **76**, 1143 (2004)
- Salvaterra, R., Chincarini, G.: *Astrophys. J.* **656**, L49 (2007)
- Salvaterra, R., Guidorzi, C., Campana, S., Chincarini, G., Tagliaferri, G.: *Mon. Not. R. Astron. Soc.* **396**, 299 (2009)
- Wang, X.-G., Liang, E.-W., Li, L., et al.: *Astrophys. J.* **774**, 132 (2013)
- Wang, F.Y., Dai, Z.G., Liang, E.W.: *New Astron. Rev.* **67**, 1 (2015). <https://doi.org/10.1016/j.newar.2015.03.001>
- Wu, S.W., Xu, D., Zhang, F.W., Wei, D.M.: *Mon. Not. R. Astron. Soc.* **423**, 2627 (2012)
- Xue, L., Zhang, F.-W., Zhu, S.-Y.: *Astrophys. J.* **876**, 77 (2019)
- Yonetoku, D., Murakami, T., Nakamura, T., et al.: *Astrophys. J.* **609**, 935 (2004)
- Yonetoku, D., Nakamura, T., Sawano, T., et al.: *Astrophys. J.* **789**, 56 (2014)
- Yu, H., Wang, F.Y., Dai, Z.G., Cheng, K.S.: *Astrophys. J. Suppl. Ser.* **218**, 13 (2015)
- Zhang, B.: *Chin. J. Astron. Astrophys.* **7**, 1 (2007)
- Zhang, B.: *CRP* **12**, 206 (2011)
- Zhang, G.Q., Wang, F.Y.: *Astrophys. J.* **852**, 1 (2018)